ADVANCED FUNCTIONAL MATERIALS
www.afm-journal.de

Highly Parallel and High-Throughput Nanoliter-Scale Liquid, Cell, and Spheroid Manipulation on Droplet Microarray

Joaquin E. Urrutia Gómez, Meijun Zhou, Nikolaj K. Mandsberg, Julian A. Serna, Julius von Padberg, Sida Liu, Markus Reischl, Pavel A. Levkin, and Anna A. Popova**

The droplet microarray (DMA) platform is a powerful tool for high-throughput biological and chemical applications, enabling miniaturization and parallelization of experimental processes. Capable of holding hundreds of nanoliter droplets, it facilitates the screening and analysis of samples, such as cells, bacteria, embryos, and spheroids. Handling thousands of small volumes in parallel presents significant challenges. In this study, we utilize the open format of the DMA for controlled, parallel high-throughput liquid manipulations using the sandwich technique. We demonstrate high-throughput medium replacement at nanoliter-scale, maintaining high cell viability on DMA for up to 7 days; for HeLa-CLL2 cells (adherent) and SU-DHL4 cells (suspension), and up to 14 days for HEK293 spheroids. Additionally, we achieve highly parallel aliquot uptake from nanoliter droplets, enabling non-destructive cell viability assessments. Furthermore, the presented method enables the parallel transfer of cell spheroids between different DMAs, allowing transfer and pooling of spheroids in seconds without damage. These advances significantly enhance the capabilities of the DMA platform, enabling long-term cell culture in nanoliter droplets and parallel sampling for high-throughput cell or spheroid manipulation. This broadens the scope of DMA's potential applications in fields such as cell-based high-throughput screening, formation of complex 3D cell models for drug screening, and microtissue engineering.

1. Introduction

Recently, droplet microarrays (DMAs) have emerged as a promising technology in cell-based assays requiring miniaturization.[1] This technology enables assays to be conducted in nanoliter volumes that are 100–1000 times smaller compared to standard formats like 96-well or 384-well plates.[2] Additionally, droplet microarrays facilitate the analysis of a larger number of samples, allowing researchers to explore a wider range of experimental conditions in a single assay. Unlike standard well plates or closed microfluidics systems, where liquids are confined within physical walls, droplet arrays are open systems where droplets are confined to predetermined planar areas by hydrophilic-superhydrophobic patterning without physical barriers. This open nature facilitates various droplet generation methods, including manual addition (dipping, tilting, and dragging) and automatic addition using specialized liquid dispensers, as well as subsequent droplet manipulation, such as movement, merging, and interconnection.[3]

The DMA (**Figure 1A**) consists of a surface-functionalized and photochemically patterned glass slide with a nano-micro rough coating featuring hydrophilic spots on a superhydrophobic background. This design allows for the formation of arrays comprising hundreds to thousands of droplets within a compact footprint of 75 mm × 25 mm. Its unique surface patterning method[4] enables the fabrication of DMAs with diverse droplet sizes, geometries, and densities, making it adaptable for various applications. The DMA has proven compatible with a wide range of biological applications, including 2D and 3D cell culturing of mammalian cells and microorganisms.[5] It has been used for applications such as anticancer drug screening, culturing induced pluripotent stem cells (iPSCs) with surface protein coatings,[6] and testing antimicrobial compounds on multi-resistant bacterial strains of clinical interest.[7] Additionally, since DMAs do not rely on gravity to confine samples but instead utilize chemical functionalization and patterned liquid adhesiveness to keep the liquid on the surface, they enable the easy generation of 3D cell culture models using the hanging drop method.[8] In this technique, the DMA is simply inverted, allowing cells to aggregate and remain suspended in the droplet, rather than settling on the surface of

J. E. Urrutia Gómez, M. Zhou, N. K. Mandsberg, J. A. Serna, J. von Padberg, S. Liu, P. A. Levkin, A. A. Popova
Institute of Biological and Chemical Systems – Functional Molecular Systems
Karlsruhe Institute of Technology (KIT)
Kaiserstraße 12, 76131 Karlsruhe, Germany
E-mail: levkin@kit.edu; anna.popova@kit.edu
J. E. Urrutia Gómez, M. Reischl
Institute of Automation and Applied Informatics
Karlsruhe Institute of Technology (KIT)
Eggenstein-Leopoldshafen, 76344 Karlsruhe, Germany
P. A. Levkin
Institute of Organic Chemistry
Karlsruhe Institute of Technology (KIT)
Kaiserstraße 12, 76131 Karlsruhe, Germany

The ORCID identification number(s) for the author(s) of this article can be found under https://doi.org/10.1002/adfm.202410355

DOI: 10.1002/adfm.202410355

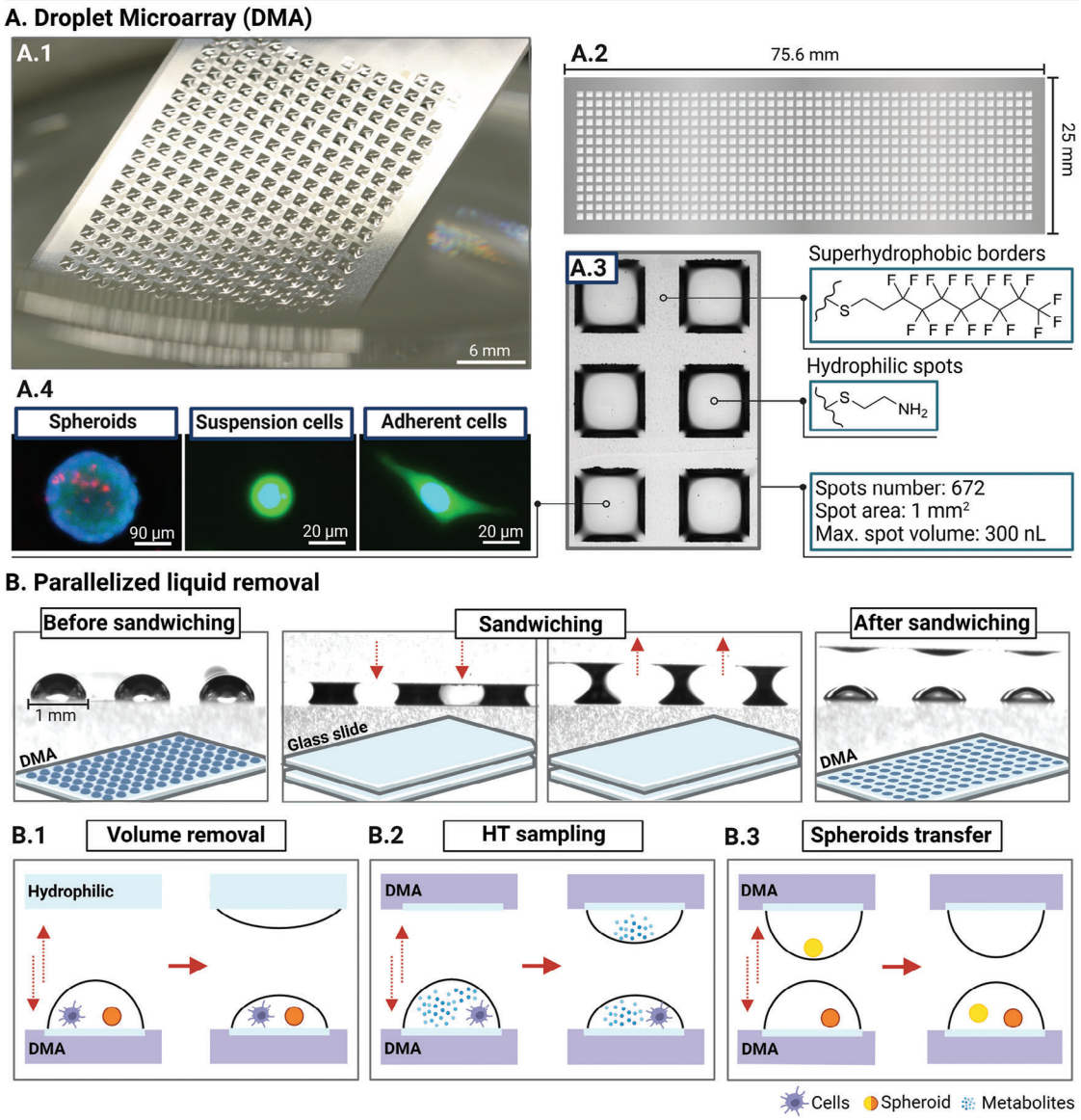

Figure 1. DMA and sandwiching strategy. A.1) Image of the DMA submerged in water showing the formation of nanoliter droplets due to its hydrophilic spots on a superhydrophobic background. A.2) DMA dimensions match those of a standard microscope slide. A.3) Microscopy image featuring 6 spots: showcasing superhydrophobic borders and hydrophilic spots within the DMA. A.4) Microscopy images capturing diverse cell culture models on DMA substrate. B) Schematic depicting the assembly of the sandwich-like structure using a DMA. The procedure is illustrated from left to right. (Before sandwiching) The initial inset shows a side view of the DMA containing 300 nL droplets, alongside an illustration showing how the droplets are positioned. This slide is hereafter referred to as the donor slide. (Sandwiching) The insets show the DMA sandwiched by a counter slide, which is referred to as the acceptor slide. When positioned 0.4 mm above the base of the droplets using an adapter, the acceptor slide contacts the droplets, forming a capillary bridge. As the acceptor slide is removed, the capillary bridge elongates until instability occurs at its neck, resulting in two isolated droplets. (After sandwiching) Side view image of the DMA post-sandwiching, showing a reduction in droplet volume. B.1.2.3) Schematic representation of the different sandwich-based applications developed in this paper. Volume removal allows to remove a portion of the droplet volume using a homogeneous surface as an acceptor slide. High-throughput Sampling (HT Sampling) employs a DMA slide as an acceptor slide, with identical dimensions to the donor slide, for liquid removal, thereby producing a copy of the donor slide. For the spheroids transfer DMA slides were used as a donor and acceptor slides to transfer spheroids between them using gravity.

the array. This makes DMAs an excellent platform for the rapid and high-throughput formation of spheroids, enabling applications such as 3D multicellular assemblies and drug screening.[9]

While DMAs present great potential for miniaturized assays, several challenges arise due to the small volume and rapid evaporation of nanoliter droplets. Critical tasks such as 1) medium exchange, 2) non-destructive sampling, and 3) cell manipulation remain difficult to perform on DMAs. While these tasks have been successfully automated in well plates using robotic pipettors, DMAs' dense array format complicates the process, especially as the number of droplets increases into thousands where sequential sample handling is unfeasible.[10] Overall, traditional

liquid handlers struggle to accommodate the high-density configuration of nanoliter arrays.[11] Nevertheless, several systems now exist that reliably dispense nanoliter droplets onto DMAs. These advancements have significantly expanded the possibilities for assays that were previously unfeasible in the early stages of this technology, enabling elegant approaches such as liquid-liquid extraction for high-throughput purification on DMAs.[12]

Although the formation of single spheroids per droplet on DMAs is well established,[13] precise and parallel droplet manipulation of thousands of nanoliter droplets can be important for various applications, such as array copying, sampling, or creating multi-spheroid structures by transfer of spheroids from droplet to droplet. Additionally, long-term maintaining of these cell cultures by frequent medium exchange is important and challenging due to nanoliter volumes.

To facilitate the efficient and simultaneous manipulation of hundreds to thousands of droplets, prior studies have utilized the sandwiching method.[14–17] This technique utilizes the open format of the DMA by placing a sufficiently hydrophilic counter slide on top, creating a sandwich-like structure. In these studies, the sandwiching method was used to add various substances or solvents to the array of open droplets—either by sandwiching the DMA with pre-printed, dried substances on a parallel surface or with a DMA containing droplets of solvent.

Here, we expand the application of the sandwiching method to achieve two primary objectives: 1) highly parallel uptake and sampling of nanoliter droplets on DMA and 2) high-throughput, non-invasive array-to-array transfer of 3D cellular structures. In our study, we used two different acceptor surfaces: coated glass slides and a second DMA slide. The hydrophilicity of the acceptor slides allows for controlled and synchronized splitting of the droplets when the acceptor surface is removed from the DMA, resulting in the droplets being divided between the two surfaces (Figure 1B). Additionally, we employed this sandwiching configuration to align droplets from different DMAs, facilitating their merging and interaction, which enables the transfer of cell content between the two DMAs. These advancements enhance the potential for high-throughput, miniaturized studies, unlocking new possibilities in areas such as drug screening, developmental biology, and advanced microtissue engineering.

2. Results and Discussion

2.1. Parallel High-Throughput Droplet Merging and Splitting Using Sandwiching

Previous studies have employed a range of methods to sandwich two glass slides, from manual handling using custom-built metal frames[15] to automated platforms for greater precision and stability.[14] However, both the automated setup and the metal frame, while precise, were bulky and impractical for routine use. Furthermore, in both cases, the technique was only used to transfer anticancer compounds by reconstituting dried compounds from one slide to another. Here, we focus on the parallel uptake of droplets and transfer their content, extending the technique's application to routine on-chip laboratory assays, primarily focused on cell culture manipulation.

To make the technique easier to employ while improving control and repeatability during slide alignment, we developed a 3D-printed adaptor incorporating a spacer that maintains the desired separation between the DMAs, determined by the spacer's height (Figure S1, Supporting Information). This adaptor was fabricated using maskless projection stereolithography with a digital light processing (DLP) 3D printer. The adaptor's open-window design allows for monitoring during the droplet manipulation process. As demonstrated in Video S1 (Supporting Information), the sandwiching adaptor was used to align two slides. First, one slide is placed on the table, followed by positioning the adaptor on top of it, and then the second slide is placed onto the adaptor. The alignment process was completed in less than a minute. To remove the top slide, either tweezers can be used, or the adaptor can simply be lifted along with the top slide. The frame structure of the adaptor provided constant visibility throughout the procedure, allowing the user to monitor and ensure successful contact of all droplets with the opposing slide.

Utilizing the designed sandwiching adaptor, first, we have investigated the droplet splitting process on DMA using a poly (2-hydroxyethyl methacrylate-co-ethylene dimethacrylate) (HEMA-EDMA) coated surface as an acceptor slide. This polymer was chosen for its highly wettable properties (static water contact angle (θ_{st}) close to 0°), making it ideal for droplet adhesion (**Figure 2A**). Upon sandwiching the droplet pinned on a planar surface, a capillary liquid bridge forms between the two surfaces. 2 Initially, when the droplets on the donor DMA slide come into contact with the acceptor slide, they form r–θ-type capillary bridges,[18] where the end of the bridge on the donor slide has a pinned triple line, while the other end on acceptor slide maintains a fixed apparent contact angle (Figure 2B.1).[19] The pinning occurs due to the DMA's high-contrast wettability pattern, which immobilizes the triple line on the hydrophilic spot perimeter, where the advancing contact angle is 168° and the receding contact angle is <5°. As they are separated again, the bridge undergoes Rayleigh instability, where surface tension drives the bridge to break into smaller droplets, minimizing surface energy. Therefore, the separation ultimately results in the formation of one droplet on each acceptor and donor slide (Figure 2B).

In case of successful splitting, the sizes of the two droplets will be determined by the neck position (i.e., the inflection point of the capillary bridge), which depends on the total volume, the wettability properties of both substrates,[20] relative substrate alignment, and the separation velocity.[21] The shape of these small capillary bridges is determined purely by surface tension rather than gravity, as the Bond number, which characterizes the relative importance of gravity compared to surface tension in liquid behavior, here is ≈0.03.[22] The estimation of volumes after the splitting of the droplets is complicated by the square footprint of hydrophilic spot, which defines the shape of cylindrical bridges. Therefore, we experimentally determined the relationship between necking point and initial volume (total volume) of the droplets (from 279 to 606 nL); Figure 2C illustrates the capillary bridges formed immediately before the droplet splits, i.e. the moment of instability, while Figure 2D plots the heights of the capillary bridge and necking point, as well as the final height of the bottom (donor) droplet after the splitting, all as a function of initial droplet volume. According to our data, we have observed two regimes in the splitting behavior of the droplets. For initial

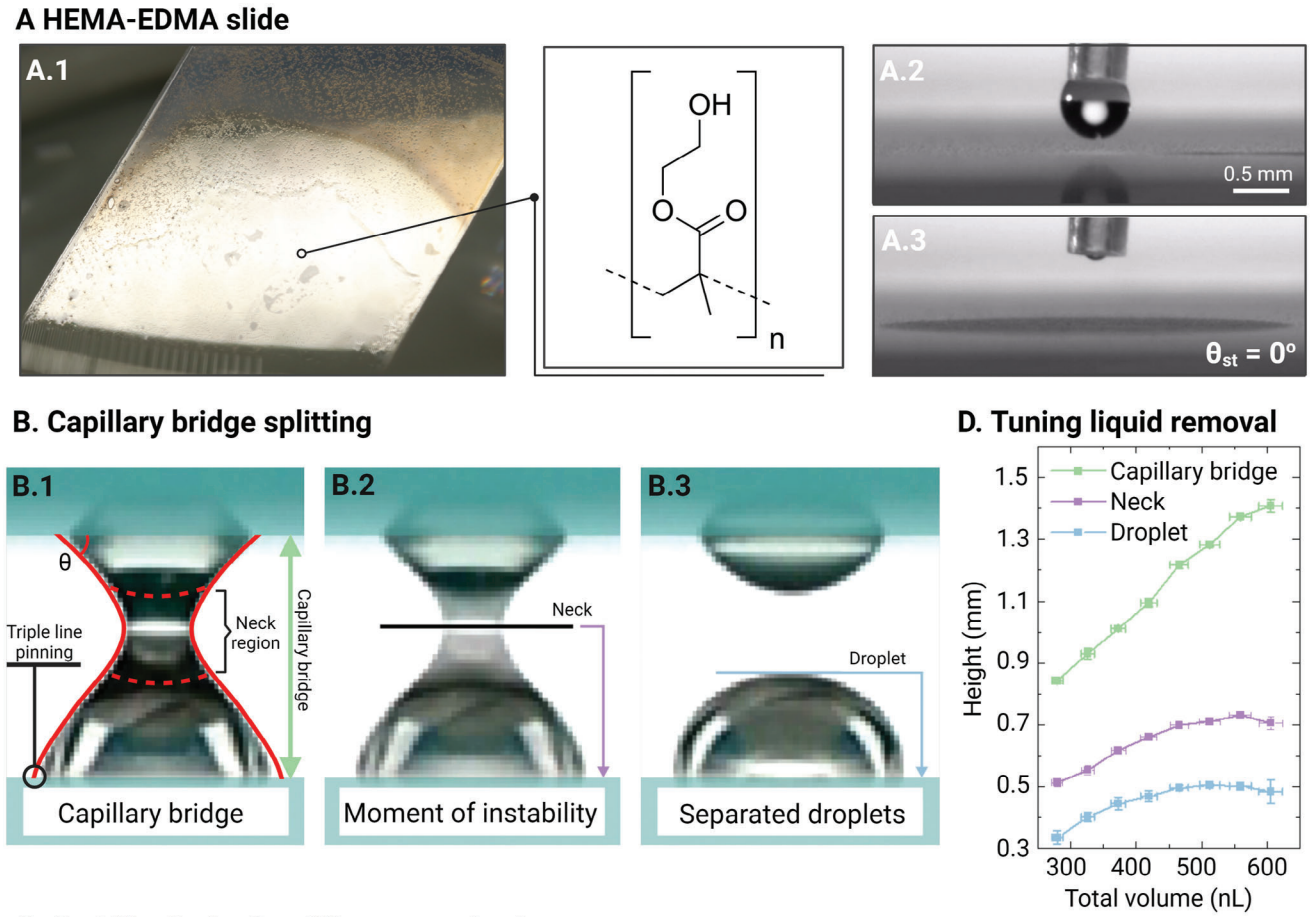

Figure 2. Analysis of volume extraction via capillary bridge instability between a DMA slide and a HEMA-EDMA polymer-coated surface. A.1) Image of the slide coated with HEMA-EDMA submerged in water showing its hydrophilicity. A.2-3) Snapshot of the deposition of a droplet on the HEMA-EDMA slide showing a static water contact angle (θ_{st}) of 0°. B) Sandwich wettability boundary conditions and capillary bridge (B.1) before, (B.2) during, and (B.3) after its division into two droplets. C) Photos of capillary bridges of different volumes immediately before instability. Scale bar 0.5 mm. D) Capillary bridge, neck, and resulting droplet height as a function of total capillary bridge volume ($n = 4$).

droplet volumes ranging from 279 to 419 nL, the final droplet height of the droplet left on the DMA after the sandwiching increases with increasing initial volume. While for larger initial volumes ranging from 466 to 606 nL, the height of remaining droplets becomes constant and therefore independent of initial droplet volume (Figure 2D). The neck height exhibits a similar plateauing, while the capillary length continuous to increase throughout the whole range of volumes ($R^2 > 0.99$). These two regimes result from an effective decoupling between the neck region and the boundary conditions imposed by the acceptor slide. This is most clearly seen by comparing capillary bridge profiles (Figure 2C; red dashed line shows the 606 nL profile overlayed on all images). Larger volumes produce nearly identical profiles, differing only in the position of the truncation, defined by the acceptor slide. In contrast, when the volume decreases, the truncation occurs closer to the neck, causing the contact angle constraints from the acceptor slide to interfere with the capillary bridge shape, shifting the necking point toward the donor slide, and ultimately reducing the final droplet size. We note that the independence at large volumes is likely to break down as the volume continues to increase and gravity begins to affect the bridge shape, potentially causing a further increase in the bottom droplet height. Overall, this shows that it is possible to control the volume fraction (see also Figure S2A, Supporting Information) taken up by changing the initial volume, but that the relationship is highly non-linear.

2.2. Parallel High-Throughput Medium Exchange Enables Long-Term Cell Culture

Without refreshing the cell medium, adherent and suspension cell cultures on the DMA platform were limited to a maximum of three days. Beyond this period, there is a significant decline in cell viability, with typically reported decreases of up to 40% by day four.[23] The main reason for this limited culture time is the challenge of simultaneously removing cell medium from 672 nanoliter droplets while avoiding sample evaporation and cross-contamination. To address this, we used a HEMA-EDMA coated glass slide to remove cell medium from droplets in parallel. As shown in Figure S2 (Supporting Information), sandwiching step with droplets of ≈300 nL results in the removal of 50% to 60% of the droplet volumes. Following this, as illustrated in **Figure 3A**, ≈15 HeLa CCL2 cells (human cervical cancer cells) were first printed in 300 nL of culture medium on each spot and subsequently incubated for 24 h in a standard cell culture incubator. Afterward, the sandwiching method was employed to remove approximately half of the spent medium from each nanoliter droplet, which was promptly substituted with 150 nL of fresh medium using a liquid dispenser (I.DOT, Dispendix GmbH, Germany). This process was performed daily for 7 days. Figure 3C illustrates the outcomes of two different cell culture conditions. Cultures with daily medium replacement displayed an exponential growth rate of 0.27 per day, calculated using the equation $Growth\ rate = \frac{ln\left(\frac{N_t}{N_o}\right)}{t}$, where N_o represents the initial cell count, N_t is the cell count at the endpoint, and t is the time in days. Notably, the growth rate per day reflects the relative change in the number of cells over time, rather than the absolute number of cells added each day. The culture subjected to medium exchange exhibited a cell viability of 80% at day 7. In contrast, cultures without medium replacement over the same period exhibited a lower growth rate of 0.20 per day, with cell viability decreasing to 25% by day 7. In the context of exponential growth, a higher growth rate indicates a faster increase in the cell population. For instance, a growth rate of 0 would signify no net increase in cell number. It is important to note that the reported growth rate is an average over the seven-day period. Although growth rates may fluctuate at different time points, this value represents the overall growth trend observed during the experiment. To assess cell proliferation while concurrently considering long-term viability, we introduced the concept of viability-adjusted growth rate (VGR), calculated as $VGR = Growth\ rate \times Viability$, where viability is expressed as the ratio of viable cells to the total cell count. This allows for the capture of growth rate and viability aspects in a single value. In this context, a VGR closer to 0 indicates unfavorable cell culture conditions. For cultures undergoing daily medium replacement, the calculated VGR was 0.21. In contrast, the control cultures without medium replacement exhibited a VGR four times lower, at only 0.05, reflecting less favorable conditions. Additionally, we demonstrated that HeLa cell culture could be extended from 7 to a maximum of 10 days by replenishing the medium every other day. As illustrated in Figure S3 (Supporting Information), this regimen resulted in a mean VGR of 0.27 (n = 2); however, the mean cell viability by the 10th day was ≈25%.

To broaden the application scope, we replicated the experiment with suspension cells, specifically SU-DHL4 (human B-cell lymphoma). As depicted in **Figure 4C**, SU-DHL4 cell cultures subjected to daily culture medium exchange exhibited a VGR of 0.10, compared to 0.08 for the control sample. Similar to the adherent cells, suspension cells subjected to medium refreshing showed a higher VGR compared to the control group, with a 25% greater increase.

Exchanging the medium of suspension cell cultures and 3D spheroids is challenging, even in plates, due to their non-adherent nature. These cells are susceptible to being washed away and lost during the medium exchange procedure. Consequently, a natural question is whether or not the sandwiching method removes suspension cells from the culture droplets. As shown in Videos S2 and Video S3 (Supporting Information), suspension cells in a droplet with sub-millimeter height, they tend to remain at the bottom. For example, in the first video, a 1.4 mm diameter spot filled with SU-DHL4 cells is being sandwiched, and it can be observed how thousands of cells settle at the base of the droplet. The video shows that these cells remain at the base and are not displaced by the flow created when the droplet splits as the top slide is removed. Similarly, in Video S3 (Supporting Information), 100 SU-DHL4 cells are sandwiched in a 1 mm^2 spot. The top glass slide is pressed several times against the droplets on the DMA to test whether the internal flow created within the droplets is capable of moving the cells. We have not observed the displacement of the cells from their original positions, as shown in the snapshots from the video in Figure 4B. The same outcome was observed with HEK293 (human embryonic kidney cells) spheroids during sandwiching, as demonstrated in Video S4 (Supporting Information). Despite repeated contact between the donor and acceptor slides, the spheroids remained in the original position retaining their morphology after the sandwiching procedure.

After evaluating the possibility of extending the culture time of 2D cell cultures, we proceeded with the medium exchange strategy on cell spheroids, which have previously been cultured for up to 7 days on the DMA platform.[13] Cell spheroids were first prepared on the DMA spots by using the hanging drop method as previously reported. After spheroids were formed, cell medium was replenished every 4 days for a period of 14 days. As depicted in Figure 4D, there was a notable 17% increase in the diameter of spheroids subjected to medium refreshment, contrasting with the control group which showed a 30% decrease in diameter. In addition, in Figure 4D.2, Hoechst and propidium iodide (PI) staining revealed a significant difference in cell viability, with notably lower viability observed in the control group. This difference between the two groups confirms the effectiveness of the strategy in preserving both the integrity and morphology of the spheroids while allowing liquid manipulation. Furthermore, unlike other approaches where hanging drop culture is extended using microchannels connected to fluid pumps,[24,25] the herein described approach offers the advantage that the spheroids are not in contact with each other, thus preserving them in individual compartments where independent experiments can be performed. Additionally, it is worth noting that the method presented in this section is the only one to date that enables medium refreshment on DMA without cross-contamination between neighboring droplets.

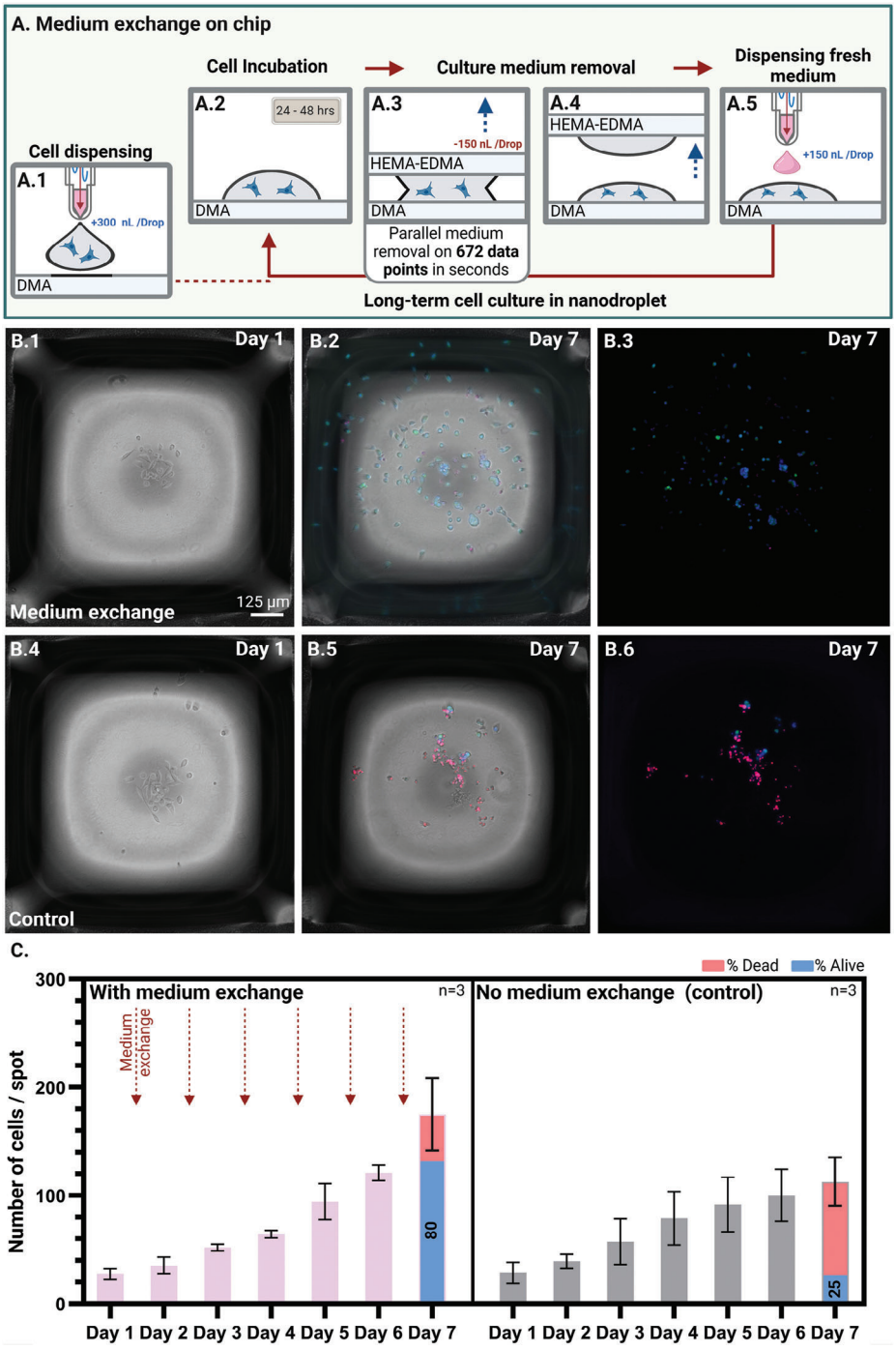

Figure 3. Extended cell culture of adherent cells (HeLa CCL2) on DMA. A) Diagram illustrating the use of the sandwiching method for prolonged cell culture in nanoliter droplets. (A.1.2) Representative images demonstrating automated dispensing of 300 nL droplets containing cells onto individual DMA spots and subsequent cell incubation for 24 to 48 h. (A.3.4.5) Images showing the use of the sandwiching method to extract 150 nL of spent medium and then add fresh medium to each droplet. This method allows for multiple cycles, thereby extending the cell culture lifetime. (B.1.4) Microscopy images of the dispensed cells on the initial day of culture. (B.2.3) Microscopy images displaying the dispensed cells on the seventh day of culture, with daily implementation of the sandwiching method to replenish with fresh culture medium. (B.5.6) Microscopy images displaying the dispensed cells on the seventh day of culture, without daily implementation of the sandwiching method. C) Graph depicting cell count over time. Pink represents cultures receiving daily fresh medium, while gray indicates cultures without fresh medium replenish for 7 days. The initial number of cells dispensed was ≈15 cells. The dotted red lines represent when the culture medium refreshing took place. The viability of cell culture on day 7 is indicated by red, representing the total percentage of dead cells, and blue, representing the total percentage of live cells. Cells were stained with Calcein (Green), Hoechst (Blue), and PI (Red) on day 7. $n = 3$.

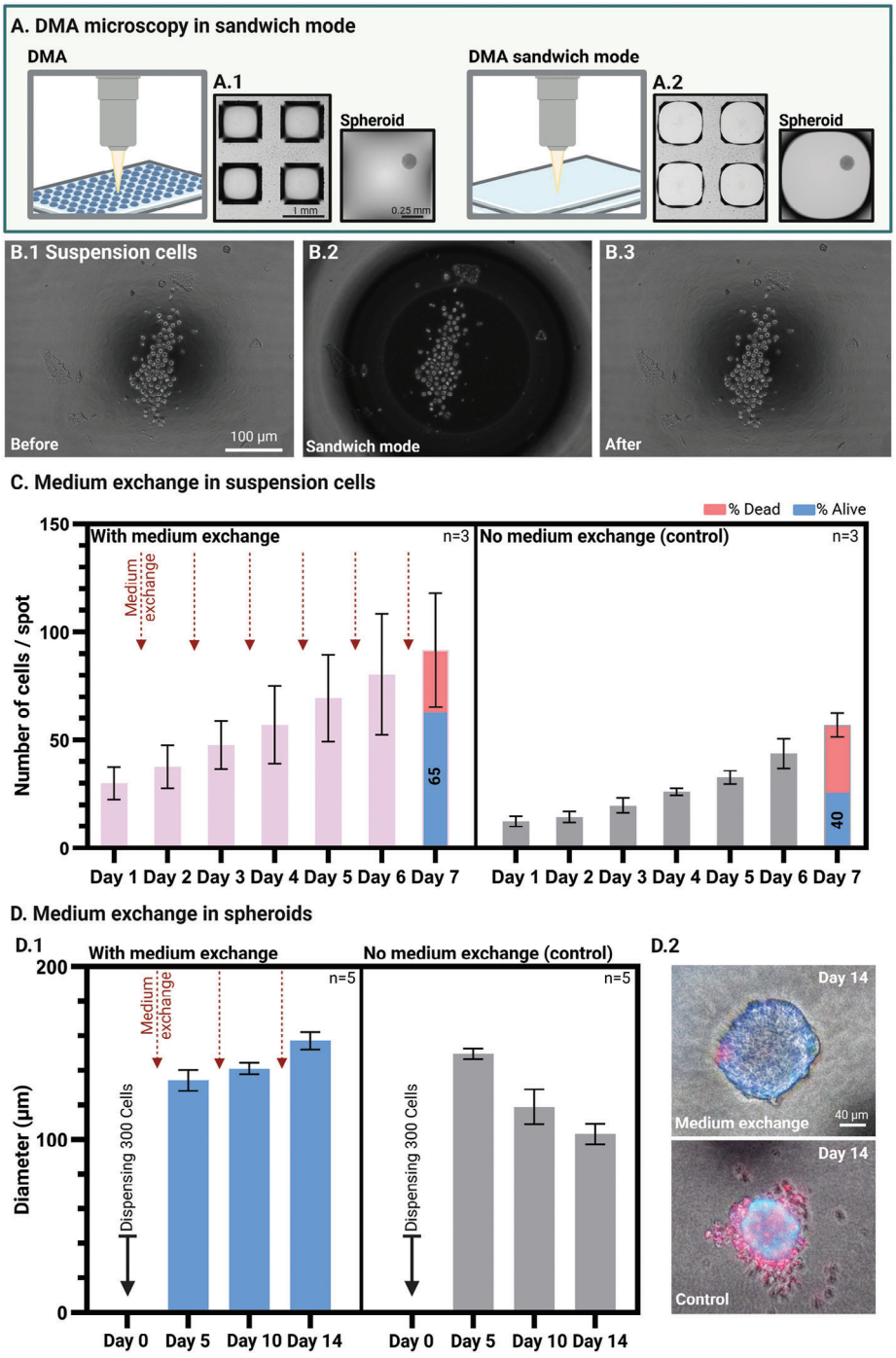

Figure 4. Extended cell culture of suspension cells (SU-DHL4) and HEK293 spheroids on DMA. A) Diagram demonstrating the improved microscopy imaging when the DMA is in sandwiching mode. (A.1) Optical microscopy image of a DMA slide featuring individual spots containing 300 nL of cell culture medium, alongside a spheroid from HEK293 cells. (A.2) Optical microscopy image of a DMA slide in sandwiching mode, displaying the previously mentioned spots, alongside the spheroid being sandwiched by the slides assessing any potential damage. (B.1.2.3) Sequential snapshots depicting suspension cells in a droplet before, during, and after the application of the sandwiching technique, demonstrating that the cells are not perturbed by this procedure. These snapshots were taken from Video S3 (Supporting Information). C) Graph depicting cell count over the culturing time. Pink bars represent cultures receiving daily medium exchange, while gray bars indicate cultures without medium exchange for 7 days. The initial number of cells dispensed was ≈15 cells per droplet. The viability of cell culture on day 7 is indicated by red, representing total dead cells, and blue, representing total live cells. Cells were stained with Calcein (Green), Hoechst (Blue), and PI (Red) on day 7. $n = 3$. (D.1) Plot of the spheroid diameter over time. Blue represents cultures receiving fresh medium every 4 days, while gray indicates cultures without fresh medium replenish for 14 days. (D.2) Images of stained spheroids on day 14. The upper image corresponds to a spheroid with addition of fresh medium every 4 days, while the bottom image corresponds to a spheroid without medium replenishment. Spheroids were stained with Calcein (Green), Hoechst (Blue), and PI (Red). $n = 5$.

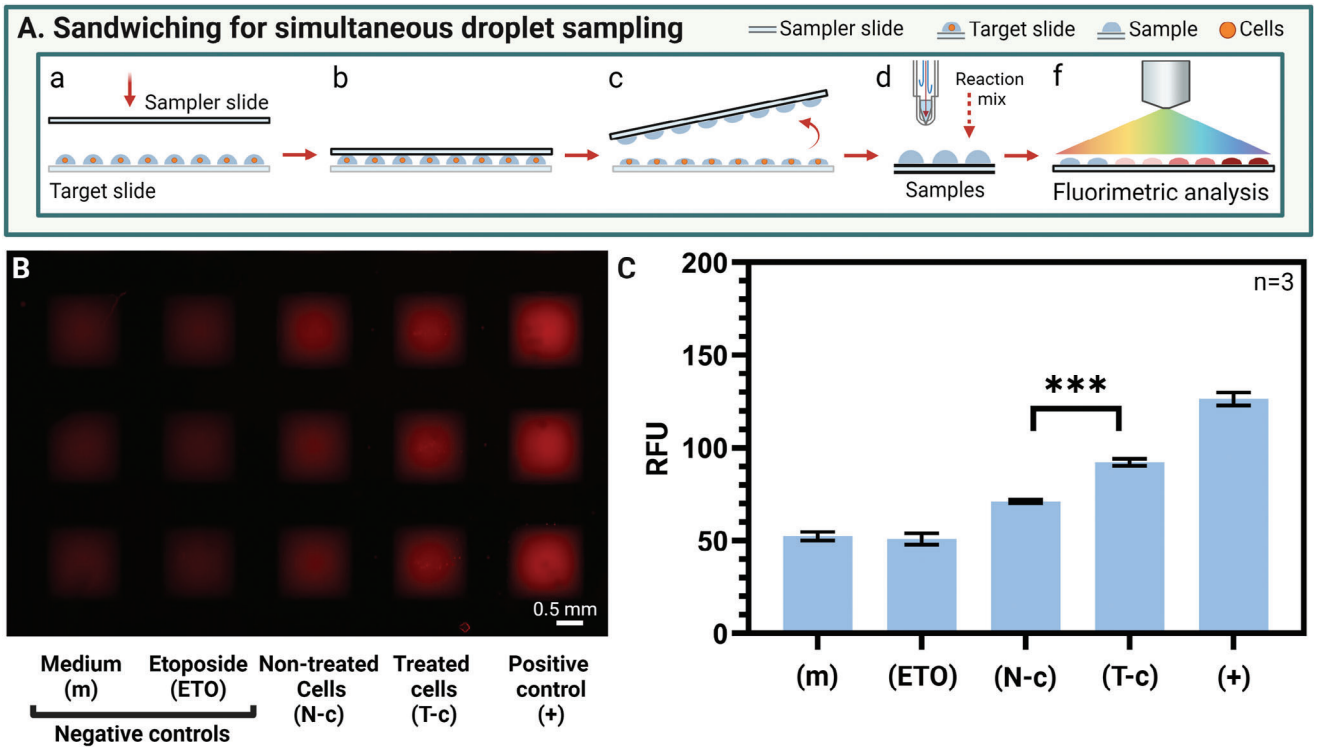

Figure 5. Sandwiching for simultaneous droplet sampling. A.a-c) Schematic illustration of step-by-step droplet sampling process from a target DMA to a sampler DMA using the sandwiching technique for subsequent analysis. B) Fluorescence microscopy image of the sampler DMA. From left to right, the columns of spots contain Medium (M), Etoposide (ETO), Non-treated cells (N-c), Treated cells (T-c), and Positive control (+), each column containing 3 replicates. C) RFU values of LDH present in different samples after being treated with 20 µM of etoposide for 48 h. LDH released into the medium was measured along with negative control (Medium and Etoposide), untreated cells (Low control), and LDH positive control. RFU (Relative Fluorescence Unit). ($^{*}p \leq 0.05$, $^{**}p \leq 0.01$, $^{***}p \leq 0.001$, $^{****}p \leq 0.0001$).

2.3. Parallel Sampling of Cell Culture Medium from Nanoliter Droplets

Sampling of conditioned cell media is important as part of non-destructive cell monitoring assays in both 2D and 3D cell cultures. In such assays, biomolecules present in the cell media can be analyzed to monitor cell health, function, and metabolic activity in long-term studies or prior to subsequent downstream analyses.[26] However, when using conventional cell culture platforms such as microwell plates, sampling media from hundreds of wells can be time-consuming and labor-intensive, even with multichannel pipettes. This process typically involves multiple pipetting steps and requires hundreds of pipette tips, making it less efficient and not a parallel single-step process. We hypothesized that the open format of the DMA in combination with the sandwiching method could allow parallel sampling of thousands of individual spots in a matter of seconds. To demonstrate this, we measured lactate dehydrogenase (LDH) levels in the medium of cultured HeLa cells as an indicator of cell viability. LDH is an enzyme that is released to the extracellular medium when the cell plasma membrane is damaged, thereby serving as a marker of cell integrity.[27] The LDH assay involves the conversion of lactate to pyruvate and nicotinamide adenine dinucleotide phosphate (NADH) by LDH, resulting in the generation of a fluorescent product (Ex/Em = 535/587 nm), the intensity of which is directly proportional to the number of dead cells. In the experiment, HeLa cells were exposed to 20 µM etoposide for 48 h, a drug commonly employed in anticancer therapies to induce cell death by interfering with DNA synthesis processes.[28] Treated cells were used as the study specimen, while untreated cells served as a comparison group. **Figure 5** illustrates the strategy employed on a 1 mm^2 spot DMA to perform the sampling of culture medium. For this, we used an identical empty DMA slide to precisely transfer the medium from individual droplets containing cells to separate compartments of accepter or sampler DMA. This approach allows for the distinct analysis of absorbed metabolites, eliminating cross-contamination between the samples.

As shown in Figure S2 (Supporting Information), the removal of volume from one DMA using another empty DMA slide is comparable to using a HEMA-EDMA coated slide. For droplets of 300 nL, ≈50% of the volume is removed. In this way, ≈150 nL of the cell medium was removed from the target DMA using the sampler DMA. Afterward, the LDH reaction mix was dispensed in the sampler DMA, and the mixture was incubated for 5 min to allow the reaction to take place and emit fluorescence (Figure 5B,C). We observed an approximate 40% increase in fluorescence in the medium from treated cells compared to untreated cells, which was equal to medium control (m) indicating 0% viability after the treatment with 20 µM of etoposide.[29] By employing this sampling strategy, it becomes feasible to extract a sample of medium from thousands of individual nanoliter

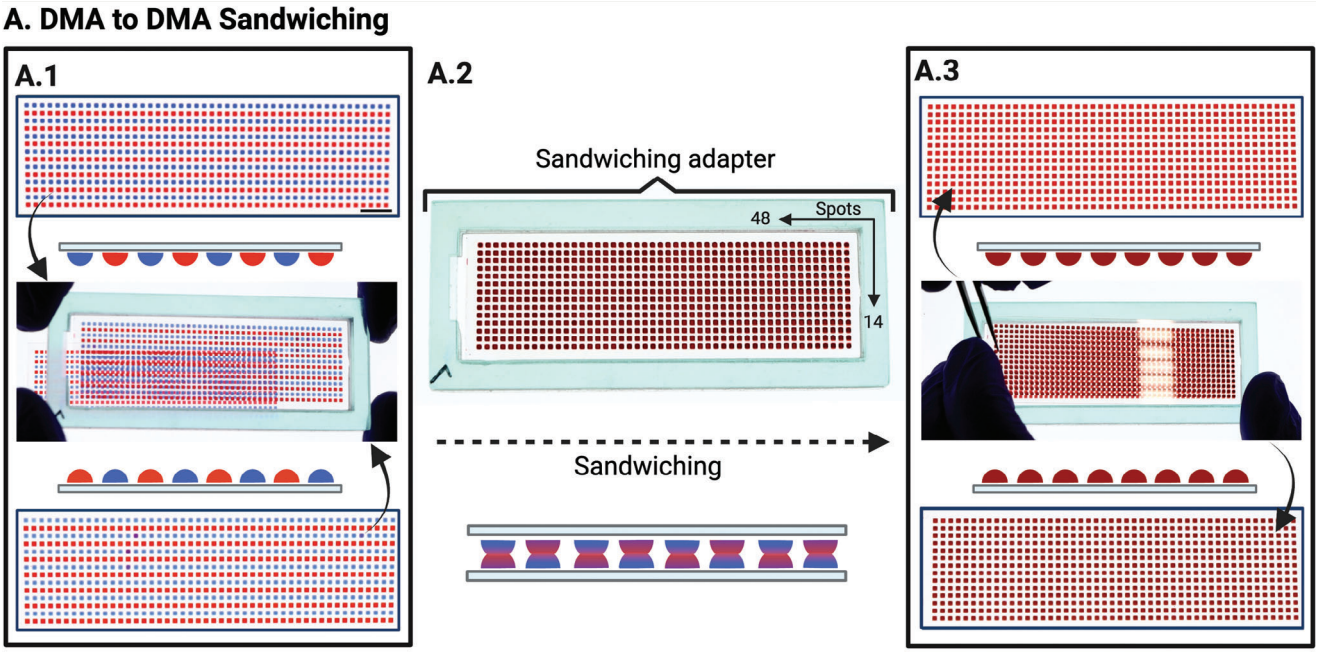

Figure 6. Sandwiching workflow for parallel merging droplets between two DMAs. A) An illustration of the sandwiching method, using DMA slides containing droplets of red and blue pencil ink as an example. (A.1) Snapshot from Video S1 (Supporting Information) showing two DMAs printed with blue and red ink droplets. The image shows how they are placed one on top of the other using an adapter. Scale bar 7 mm. (A.2) Snapshot showing both DMAs being sandwiched together. (A.3) Snapshot showing the result of the sandwiching process, demonstrating that all droplets successfully merged with their counterparts without any cross-contamination between neighboring droplets. In the image, the top DMA is being removed from the other using tweezers.

droplets simultaneously in a single step. Additionally, creating a direct copy of the target slide on the sampler slide reduces human error caused by manual pipetting and facilitates immediate analysis of each sample without prior labeling or separation into different vessels. Overall, the parallelized sampling through sandwiching proves to be a robust approach when working with the DMA. It offers a straightforward method to perform control screens in nanoliter-scale cultures, as well as the potential to screen molecules of interest produced in the culture medium, such as recombinant proteins or enzymes.

2.4. Parallel Manipulation of Cell Spheroids

The manipulation of cell aggregates such as spheroids is of great interest in the fields of cell biology and tissue engineering. The ability to construct multicellular 3D structures makes it possible, for example, to study tissue morphogenesis[30] or to create advanced models of diseased tissues.[31] Current strategies to manipulate 3D cell aggregates rely mainly on aspiration systems that collect and transport the aggregates through gel-like or liquid media[31,32] as well as techniques utilizing magnetic levitation and assembly.[33,34] Additionally, rotating or dynamic cultures are also employed for this purpose.[35,36] However, these approaches are limited due to their reliance on complex instrumentation and their low throughput. To overcome these limitations, we employed the sandwiching method to transfer spheroids from one DMA to another, by positioning one slide above the other, as shown in **Figure** 6A. This method relies on gravity to ensure the spheroids move from the top DMA to the bottom.

To achieve this, we first tested the sandwiching adaptor for mixing droplets between two DMAs. Each DMA was printed with 250 nL droplets of red and blue dye in alternating parallel lines (Figure 6A.1). As demonstrated in Video S1 (Supporting Information), the sandwiching process began with one DMA placed on a flat surface. The sandwiching adaptor was then positioned on top, followed by placing another DMA on the adaptor to achieve precise alignment. After the droplets merged, the top DMA was removed using tweezers, followed by the removal of the adaptor from the DMA on the surface. The result showed that all droplets from both DMAs successfully merged and mixed, without any fusion or cross-contamination between adjacent droplets within the DMA (Figure 6A.3). The entire process of sandwiching and splitting of two DMA containing 672 droplets each took approximately one minute.

By employing the same workflow, we smoothly transferred single spheroids from 1 mm^2 spots containing in 300 nL of culture medium to a bigger DMA format featuring 2.8 mm diameter spots with 5 µL of medium (**Figure** 7A.4). Similarly, Figure 7B illustrates the controlled transfer of spheroids from 672 individual 1 mm^2 spots on one DMA to an identical DMA containing spheroids. The process begins with the acceptor slide containing single spheroids per droplet stained with Hoechst (blue) in 250 nL droplets (Figure 7 B.1). Simultaneously, the donor slide also contains spheroids in 250 nL, but alternately located on the DMA and stained with Calcein (green) for better tracking (Figure 7B.2). The transfer process continues as the donor slide is placed on top

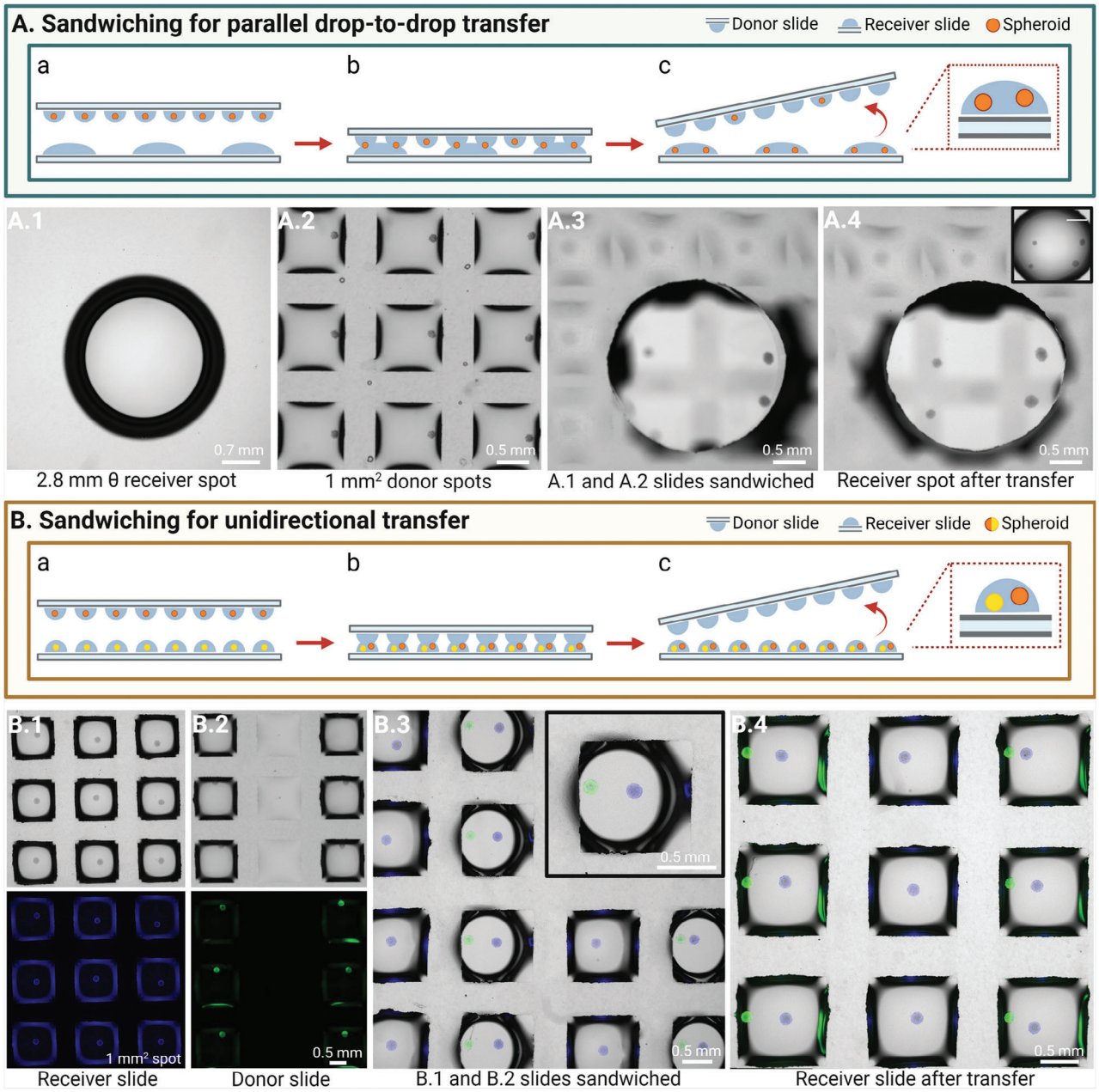

Figure 7. Sandwiching for parallel drop-to-drop transfer of cellular spheroids. A.a–c) Step-by-step schematic representation of workflow of the transfer of an object from one DMA to another DMA through the utilization of the sandwiching method. (A.1) Spot with a diameter of 2.8 mm, containing 5 µL of culture medium. (A.2) 1 mm^2 spots containing 300 nL of culture medium and HEK293 spheroids. (A.3) Image of the target spot beneath the donor spots containing the spheroids. (A.4) Image depicting successful transfer of four spheroids from the donor slide to the receiver slide using the sandwiching method. The accompanying image in the upper right corner displays the target spot post-transfer. Scale bar 1.4 mm. B.a–c) Schematic illustrating the step-by-step process of transferring multiple objects from one DMA to another DMA, which already contains an object, using the sandwiching method. (B.1) Image showing a 1 mm^2 DMA containing spheroids stained with Hoechst (blue) in 250 nL droplets. (B.2) Image showing a 1 mm^2 DMA containing spheroids stained with Calcein (green) placed alternately in 250 nL droplets. (B.3) Image of the receiver slide beneath the donor slide. The top right image shows an enlarged image of a spot being sandwiched. (B.4) Final arrangement of spheroids achieved by the sandwiching method.

of the receiver slide (Figure 7B.3), allowing controlled transfer of the spheroids from one spot to another, driven by gravity. The result is a slide featuring spheroids with different stains, sharing the same spot and arranged in alternating patterns, demonstrating the controllability of the process (Figure 7B.4). Videos S5 and S6 (Supporting Information) provide visual evidence of the gentle handling method, ensuring that spheroids are transferred safely between DMAs without compromising their integrity or requiring additional intervention. Moreover, in our approach, unlike methods where spheroids from hanging droplets are transferred only once to cell culture dishes[37] or imaging plates,[38] transfers can be performed multiple times.

2.5. Parallel Addition of Multiple Spheroids to Nanoliter Droplets and their Fusion to Cell Assembloids

To emulate the complexity of natural tissues, artificial multicellular systems have been developed to mimic the spatial organization and geometry of different cell types within a 3D microenvironment.[39] These systems are often constructed using "building blocks",[40] such as cell sheets,[41] organoids,[42] and spheroids,[43] which are assembled into well-defined structures.

However, many existing methods for fabricating these complex 3D cellular systems require sophisticated equipment and are not conducive to high-throughput applications. Techniques like directed assembly and remote assembly, while effective, often involve manual processes or specialized tools that limit scalability and introduce potential challenges in maintaining cell viability.[44–47] Additionally, methods involving cell-laden hydrogels[48] or scaffold-based approaches[49] may suffer from low cell density or unwanted interactions with the biomaterials used.

A recent strategy introduced by Cui and colleagues utilized the open format of the DMA to achieve controlled merging of spheroids in neighboring droplets, demonstrating the creation of multi-spheroid architectures with controllable geometries.[8] While this scaffold-free approach could be potentially automated, it is limited in that it only utilizes spheroids from adjacent droplets within the same DMA, thereby reducing the overall number of spheroids available for multi-spheroid structure creation. To increase throughput in forming multi-spheroid architectures on DMAs, we employed the sandwiching technique, allowing additional spheroids from external DMAs to be added into each droplet. This method enables the formation of thousands of droplets, where each droplet contains customized number of individual spheroids, which can be then fused to complex 3D cell assembloids.

To form these structures in each individual spot, we began by forming HEK293 spheroids on three separate DMAs, each containing 672 droplets. As shown in **Figure** 8A and depicted in Video S7 (Supporting Information), we used unidirectional transfer with the sandwiching technique to sequentially transfer the spheroids onto a single DMA. This process first resulted in spheroid pairs with a success rate of 95% (Figure 8A.2), followed by triplets with a success rate of 90% (Figure 8A.3). Subsequently, the DMA was inverted, and the hanging drop technique was applied for 72 h, promoting the merging of spheroids into larger, more complex multicellular structures (Figure 8C.1).

Once the merging process is complete, the newly formed multi-spheroid architectures can either be maintained on the DMA for further studies, such as drug screenings or transferred to other platforms for additional applications. To demonstrate the potential of the harvesting process and confirm that the spheroid structures remained intact, we transferred the triple spheroids from the DMA to a well plate. The DMA was placed on the surface of a Petri dish containing cell medium, allowing gravity to facilitate the rapid transfer of the multi-spheroids in a single, seamless step (Figure 8Cc). Once settled, the supernatant was removed, and the spheroids were pooled and relocated to a well plate using standard pipetting techniques (Figure 8C.2).

The assembly of spheroid structures using the sandwiching method allows for the combination of different cell types, enabling the merging of spheroids composed of distinct cell types into unified, hetero-spheroidal structures. Additionally, it facilitates the integration of both 2D and 3D cultures within a single spot, further enhancing the versatility of the technique (Figure S4). This approach holds significant potential for mimicking the complex cellular interactions and spatial organization found in native tissues, offering greater flexibility in modeling multi-spheroid systems.

3. Conclusion

Our study has advanced the use of droplet microarray (DMA) technology across a range of miniaturized assays by demonstrating improved techniques for high-throughput and parallel manipulations of nanoliter droplets. By employing the sandwiching method for parallel high-throughput medium exchange, we successfully extended the on-chip cell culture duration of both adherent (HeLa-CLL2) and suspension cells (SU-DHL4) to 7 days, as well as HEK293 spheroids to 14 days, while maintaining high cell viability. Importantly, this method ensured that suspension cells and spheroids were not displaced during the process, highlighting its effectiveness in maintaining cell positioning and integrity. This approach also enables high-throughput sampling for non-destructive cell monitoring assays, such as the LDH assay, without disrupting ongoing cell cultures. Additionally, we demonstrated the use of droplet merging across different DMA formats, allowing for precise parallel array-to-array transfer of cell spheroids. This controlled manipulation of spheroids underscores the potential of DMA in creating 3D cellular building blocks by enabling the formation of multi-spheroid architectures in a parallel and high-throughput way. By combining spheroids into single nanoliter droplets and subsequently fusing them into larger structures, these constructs can be used both for on-chip screening and for subsequent collection and further analysis or tissue engineering. These advances highlight the versatility of DMA to adapt to complex miniaturized assays that were challenging or impossible before. This work builds toward future applications in drug development, cell-based high-throughput screening, and tissue engineering on DMA, marking a significant advancement in the capabilities of lab-on-a-chip technologies.

4. Experimental Section

Design of Sandwiching Adapter: An alignment frame was designed and fabricated to facilitate the alignment and sandwiching of the DMA slides. This frame was designed to hold the slides in place, preventing any movement during the sandwiching process. It ensured precise alignment of both slides in the XY-plane relative to each other, guaranteeing accuracy during the procedure without the need for adjustments. The frame has a spacer to create a distance between the slides in the Z-axis, allowing for consistent sandwiching with a predetermined distance of 0.4 mm between the slides (when using 672 spots DMA). Additionally, the design ensured compatibility with microscopy by maintaining no distance between the bottom surface of the frame and the lower DMA slide. This feature enabled direct microscopy within the frame, facilitating observation and analysis (Figure S1, Supporting Information). This alignment frame was designed with Autodesk Fusion 360 (Autodesk, USA) and sliced on the Chitubox slicer (CBD Technology Co., China). The chosen printing parameters were a base layer exposure time of 20 s for the first 5 layers and a body layer exposure time of 2.5 s. The chosen layer height was 50 µm per

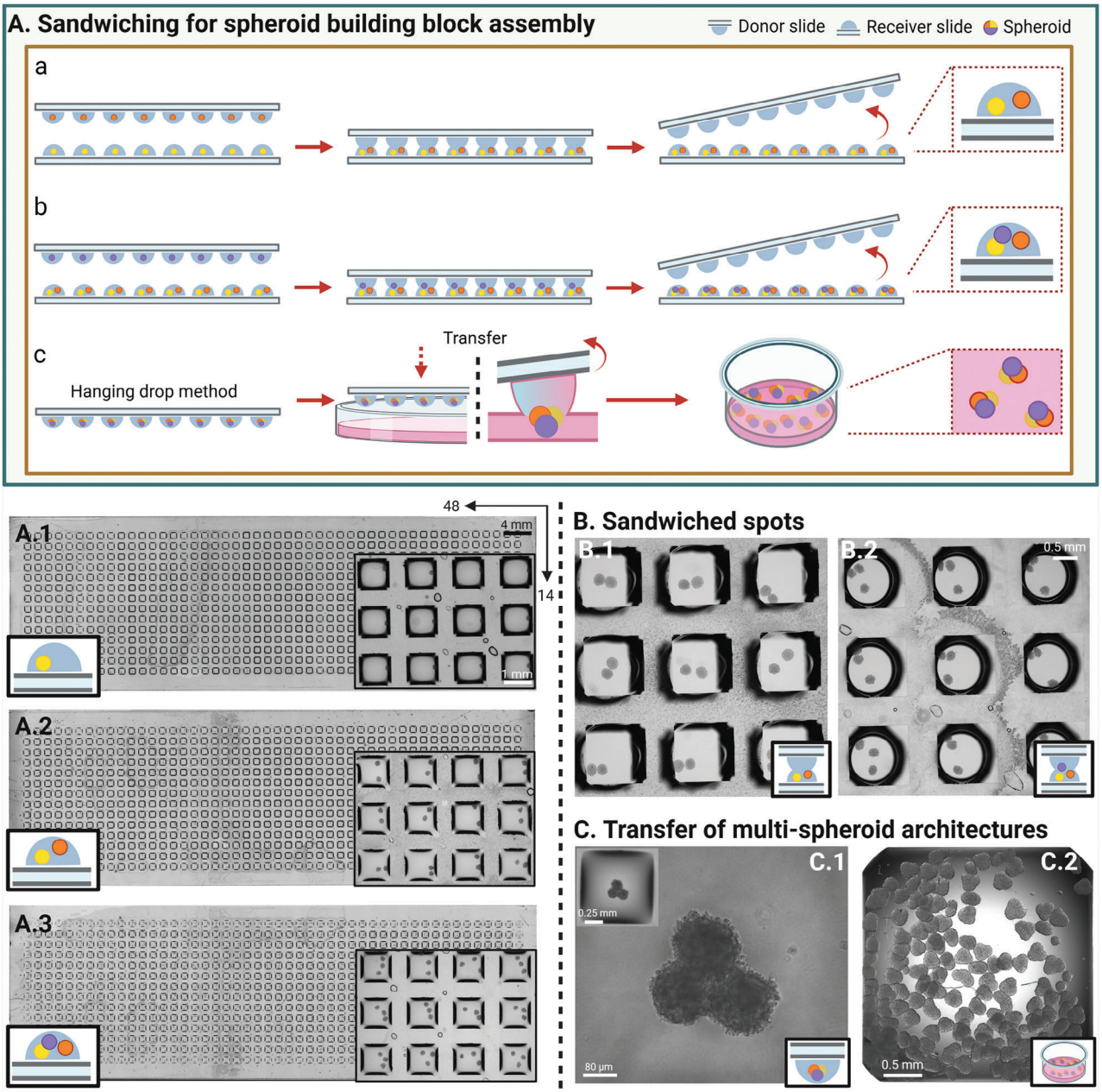

Figure 8. Sandwiching for formation and assembly of multi-spheroids cellular architectures. A.a–c) Step-by-step schematic representation of the workflow of transferring spheroids from one DMA to another DMA using the sandwich method. (A.1) 672-spot DMA, each containing a single HEK293 spheroid; inset on the right shows a magnified view of 12 spots. (A.2) DMA from image A1 after the transfer, now containing two HEK293 spheroids per spot; inset on the right shows a magnified view of 12 spots. (A.3) DMA from image A.1 after the second transfer of spheroids, showing three HEK293 spheroids per spot; inset on the right shows a magnified view of 12 spots. B1 and 2) Images obtained during the sandwiching of spots, showing how spheroids are transferred, resulting in spheroids pairs (B1) and triplets (B2). (C.1) Image showing a single spot containing three spheroids fused after 72 h. of incubation using the hanging drop method. (C.2) Image showing multi-spheroid architectures collected from a DMA and transferred to a well of a 384-well plate.

layer. The model was positioned upright on the build plate. Its Y-Z face was placed parallel to the build plate, with the X-axis vertical and perpendicular to the build plate. (X = Width, Y = Length, Z = Thickness) The DLP 3D printer used for fabrication was the Anycubic Photon D2 (Anycubic, China) with Siraya Tech Blu-Tough resin (Siraya, Taiwan). After printing, the model was washed in 70% ethanol for 10 min to remove uncrosslinked resin and finally post-cured in 405 nm light for 20 min (Anycubic Wash and Cure 3.0 (Anycubic, China)) to ensure a high and homogeneous degree of crosslinking throughout the model.

Preparation of HEMA-EDMA Slides: An uncoated Nexterion glass slide (Schott AG, Germany) underwent activation using a UVO cleaner (Jetlight Co. Inc., CA) for 10 min. Following activation, 150 µL of a

modification mixture containing 20% 3-(trimethoxysilyl)propyl methacrylate in ethanol was applied onto the slide, which was then covered with another activated glass slide. The solution was evenly distributed between the two slides, ensuring the removal of all bubbles, and allowed to react for 30 min. This functionalization process was repeated twice, followed by washing with acetone and drying with a nitrogen gun. The nanoporous poly(2-hydroxyethyl methacrylate-co-ethylene dimethacrylate) (HEMA-co-EDMA) polymerization mixture was prepared with the following components: 24 wt% 2-hydroxyethyl methacrylate (HEMA), 16 wt% ethylene dimethacrylate (EDMA), 12 wt% 1-decanol, 48 wt% cyclohexanol, and 0.4 wt% 2,2-dimethoxy-2-phenylacetophenone (DMPAP). Subsequently, 15–30 µL of the polymerization mixture was pipetted onto a fluorinated glass slide, and a modified glass slide was placed on top, allowing the mixture to spread evenly without forming air bubbles. These sandwich-like slides were then exposed to UV radiation (260 nm wavelength) for 20 min at an intensity of 10 mW cm^{-2}. After irradiation, the slides were separated and washed with ethanol, followed by immersion in ethanol for several hours.

Sterile Handling of DMA for Cell Culture Assays: To ensure sterility during all experimental procedures, the DMA was handled exclusively under clean benches. DMA chips were placed inside sterile Petri dishes with closed lids when transferred out of the clean bench and cultured in standard cell culture incubators. This ensured that the cells were handled in the same manner as those cultured in traditional Petri dishes, minimizing the risk of contamination during transportation and incubation.

All procedures involving cell printing were also performed inside the clean bench to ensure that the dispensing process was carried out under sterile conditions. For illustrative purposes, some operations, such as the sandwiching technique demonstration, were performed outside the clean bench and under a microscope for video recording. However, for routine experimental procedures, the sandwiching process and all other essential steps were performed entirely within the clean bench to always ensure sterility.

Liquids and Cell Dispensing: The pressure-based non-contact liquid dispenser, I-DOT One (Dispendix GmbH, Germany), was utilized for dispensing liquids and cell suspensions at specified cell densities. DMA slides (catalog numbers: G-np-102, G-np-201, and G-np-202) were procured from Aquarray GmbH (Eggenstein-Leopoldshafen, Germany). To prevent droplet evaporation during printing, a humidity level of 70% was maintained via an integrated humidifier.

Cell Culture: HeLa CCL2 and HEK 293T cells were cultured in Dulbecco's Modified Eagle Medium (DMEM) (Gibco, Life Technologies, Germany), supplemented with 10% fetal bovine serum (Gibco, Life Technologies, Germany) and 1% penicillin/streptomycin (Life Technologies, USA). Cells were split every 2–3 days until a cell density of 2×10^5 cells mL^{-1} was achieved.

Cell Culture on DMA: Before seeding cells on DMA, slides were sterilized with ethanol for 10 min and allowed to dry for 45 min under a clean bench. The cells were then dispensed onto the DMA at a density of 5×10^4 cells mL^{-1} (≈15 cells per drop) in 300 nL per spot. Subsequently, the DMA was placed in a cell incubator. To prevent evaporation during culture, a wet humidifier pad was inserted into the lid of the Petri dish, and the Petri dish was filled with 10 mL of PBS.

3D Cell Culture on DMA: To minimize cell adhesion on the DMA, each spot on the DMA slide was coated with 50 nL of Anti-Stick Rinse Solution (Stemcell Technologies Inc., Canada). Before coating, the DMA slides were immersed in ethanol for 10 min to ensure their sterility. Afterward, the DMA slides were placed on a clean bench to dry for 10 min. Subsequently, the slide spots were primed with 100 nL of anti-adhesion rinsing solution using the I-DOT One non-contact liquid dispenser. Following this, the DMA slides were again left to dry on a clean bench for another 10 min before being used for 3D cell culture.

For 3D cell culture, 200 nL droplets containing a suspension of HEK 293 cells at a density of 1×10^6 cells mL^{-1} (≈200 cells per droplet) were dispensed onto the DMA. To facilitate 3D spheroid formation, the DMA slide was immediately inverted after printing and placed on a specially designed 3D printed table, allowing the cell culture inside to form "hanging droplets".[5] The cells were then cultured for 48 h to form spheroids. To prevent evaporation during culture, a wet humidifier pad was inserted into the lid of the Petri dish, and the Petri dish was filled with 10 mL of PBS.

Cell Growth and Viability Study: Cell viability was assessed by staining with Hoechst 33 342 (5 µg mL^{-1}) (Invitrogen, USA), propidium iodide (PI, 5 µg mL^{-1}) (Invitrogen, USA), and Calcein AM (5 µg mL^{-1}) (Invitrogen, USA), each diluted in PBS. A volume of 50 nL was added to each spot of DMA, and the samples were incubated at 37 °C in the dark for 10 min. After incubation, cells were imaged using a Keyence BZ-X810 microscope (Keyence, Japan). The captured images were analyzed using ImageJ/Fiji (National Institutes of Health, USA) to quantify the number of life (Calcein AM-positive) and dead (PI-positive) cells. The number of viable cells was calculated as the total number of live cells (total cells minus dead cells) divided by the total number of cells.

Parallel Medium Replenishment: The HEMA-EDMA slide underwent sterilization using 70% alcohol and was left to air-dry under a clean bench for ≈10 min. Subsequently, the DMA slide containing cells was secured beneath the sandwiching adapter, while the HEMA-EDMA slide was positioned above it, forming a "sandwich" structure with the DMA slide and droplets in between. Gentle pressure applied to the HEMA-EDMA facilitated the transfer of culture medium from the DMA with cells to the HEMA-EDMA slide. Afterwards, the DMA was placed on the I-DOT One non-contact dispenser to add 150 nL of medium on top. Finally, it was returned to the petri dish containing the humidity pads and taken to the cell incubator.

Parallel Manipulation of Cell Spheroids: Cell spheroids were cultured on two DMA plates using the experimental approach described previously. One DMA plate was positioned below the sandwiching adapter, while the other was placed above it, enabling the droplets from both DMA plates to come into contact. This setup facilitated the transfer of cells from the DMA plate positioned on top to the one secured below, driven by gravity.

Collection of Spheroids: Following incubation, the merged spheroids were transferred into a 10 cm culture dish containing 10 mL of medium. The DMA was carefully placed with the side containing the spheroids facing the liquid surface of the medium. The DMA was gently placed by hand onto the medium's surface, allowing the spheroids to pass from the droplets on the DMA into the dish by gravity within seconds. After waiting for the spheroids to settle, the supernatant was carefully removed. The spheroids were then transferred into the wells of a 384-well plate using a 1 mL pipette for further observation.

Parallel Sampling of Cell Culture Medium: Using the I-DOT One non-contact dispenser, 300 cells were seeded in 300 nL droplets across 672 spots on a DMA slide, with Etoposide (Selleckchem, USA) added to achieve a final concentration of 20 µM. The slide was then placed in a Petri dish containing humidity pads and transferred to the cell incubator for a 48-h incubation period. The experimental setup included negative controls (cells only), samples (cells with etoposide treatment), a drug-only control (20 µM etoposide), a medium-only control, and a positive control group, each with three replicates. After 48 h, the LDH positive control (Abcam, UK) was prepared and applied in 300 nL to the DMA, consisting of 100 µL culture medium mixed with 2 µL of LDH positive control solution. Subsequently, a new DMA was prepared for medium removal using the sandwich method, followed by the addition of the LDH reaction mix (Abcam, UK), prepared according to the provider's instructions. The Petri dish within the humidity chamber was covered with foil and incubated for 5 min before imaging with a Keyence BZ-X810 microscope (Keyence, Japan) to assess the results.

Automated Imaging and Image Analysis: The DMA slide was placed in a four-well plate (Thermo Scientific, USA), which was fixed in a standard microtiter plate holder for microscopy. Imaging was performed with the Keyence BZ-X810 microscope (Keyence, Japan). The stitching function was used to image the entire slides. Z-stacks of 50 slices were made to consider cells in suspension in slightly different focal planes, as well as spheroids. Images of each spot were taken at 10× and 20× magnification, brightfield, and fluorescence. The image analysis, such as cell counting and fluorescence detection, was carried out using ImageJ/Fiji (National Institutes of Health Inc, USA) and the software Gridscreener.[50]

Droplet Height Measurement: Droplet height measurements were conducted using a DSA25 Drop Shape Analyzer (Krüss, Germany). Initially, different volumes of deionized water were dispensed over the spots of a DMA. The DMA with the droplets was then placed on the platform of the analyzer, and the liquid removal method was carried out and recorded by the instrument. Subsequently, measurements of droplet height were taken manually using ImageJ/Fiji (National Institutes of Health Inc, USA) before and after the process.

Statistical Analysis: The measurement error for Supplementary Figure S1 (Supporting Information) was assessed by manually taking 10 measurements of a sample with predetermined drop height and length, respectively, using ImageJ/Fiji (National Institutes of Health Inc, USA). The confidence interval (95%; 1.960 $\sigma_{\bar{x}}$) was calculated using the values of the mean and standard deviation of the experimental samples taken on each case. The droplet heights were transformed using the geometric approximation described by Wu et al.[51] using RStudio: Integrated Development Environment for R (Posit Inc, USA). The calculations and plots were computed using GraphPad Prism (Dotmatics Inc, USA).

Supporting Information

Supporting Information is available from the Wiley Online Library or from the author.

Acknowledgements

J.E.U.G. and M.Z. contributed equally to this work. The authors gratefully acknowledge the funding sources that made this work possible: DFG (Heisenbergprofessur Projekt number: 406232485, LE 2936/9-1), the Impuls und Vernetzungs fonds der Helmholtz-Gemeinschaft, Heidelberg and Karlsruhe cooperation program HEiKA, the German Academic Exchange Service (DAAD), and China Scholarship Council (CSC). N.K.M. was funded by an Internationalization Fellowship from the Carlsberg Foundation (CF21-0614). N.K.M., J.V.P., S.L and P.A.L. thank the 3DMM2O Excellence Cluster (2082/1-390761711).

Open access funding enabled and organized by Projekt DEAL.

Conflict of Interest

The authors declare the following potential conflicts of interest with respect to the research, authorship, and/or publication of this article: in addition to being employed by the Karlsruhe Institute of Technology, A.A.P. and P.A.L. are (since March 2018) shareholders of Aquarray GmbH. J.E.U.G., M.Z., N.K.M., J.S., J.V.P., S.L., and M.R. declare that there is no conflict of interest regarding the publication of this article.

Data Availability Statement

The data that support the findings of this study are available at Radar4KIT (https://radar.kit.edu/radar/de/home)

Keywords

droplet microarray, miniaturization, parallelization, sandwiching, spheroids

Received: June 13, 2024
Revised: September 21, 2024
Published online:

[1] W. Feng, E. Ueda, P. A. Levkin, *Adv. Mater.* **2018**, *30*, 1706111.
[2] L. Du, H. Liu, J. Zhou, *Microsyst. Nanoeng.* **2020**, *6*, 33.
[3] R. Strutt, B. Xiong, V. F. Abegg, P. S. Dittrich, *Lab Chip* **2024**, *24*, 1064.
[4] W. Feng, L. Li, E. Ueda, J. Li, S. Heißler, A. Welle, O. Trapp, P. A. Levkin, *Adv. Mater. Interfaces* **2014**, *1*, 1400269.
[5] H. Cui, T. Tronser, X. Wang, J. Wesslowski, G. Davidson, A. A. Popova, P. A. Levkin, *Droplet* **2023**, *2*, 39.
[6] Y. Liu, S. Bertels, M. Reischl, R. Peravali, M. Bastmeyer, A. A. Popova, P. A. Levkin, *Adv. Healthcare Mater.* **2022**, *11*, 2200718.
[7] W. Lei, A. Deckers, C. Luchena, A. Popova, M. Reischl, N. Jung, S. Bräse, T. Schwartz, I. K. Krimmelbein, L. F. Tietze, P. A. Levkin, *Adv. Biol.* **2022**, *6*, 2200166.
[8] H. Cui, X. Wang, J. Wesslowski, T. Tronser, J. Rosenbauer, A. Schug, G. Davidson, A. A. Popova, P. A. Levkin, *Adv. Mater.* **2021**, *33*, 2006434.
[9] A. A. Popova, M. Reischl, D. Kazenmaier, H. Cui, T. Amberger, P. A. Levkin, *SLAS Technol.* **2022**, *27*, 44.
[10] J. E. U. Gómez, R. E. l. K. E.l. Faraj, M. Braun, P. A. Levkin, A. A. Popova, *SLAS Technol.* **2024**, *29*, 100118.
[11] G. Du, Q. Fang, J. M. J. den Toonder, *Anal. Chim. Acta* **2016**, *903*, 36.
[12] J. J. Wiedmann, Y. N. Demirdögen, S. Schmidt, M. A. Kuzina, Y. Wu, F. Wang, B. Nestler, C. Hopf, P. A. Levkin, *Small* **2023**, *19*, 2204512.
[13] A. A. Popova, T. Tronser, K. Demir, P. Haitz, K. Kuodyte, V. Starkuviene, P. Wajda, P. A. Levkin, *Small* **2019**, *15*, 1901299.
[14] A. A. Popova, S. M. Schillo, K. Demir, E. Ueda, A. Nesterov-Mueller, P. A. Levkin, *Adv. Mater.* **2015**, *27*, 5217.
[15] A. A. Popova, C. Depew, K. M. Permana, A. Trubitsyn, R. Peravali, J. Á. G. Ordiano, M. Reischl, P. A. Levkin, *SLAS Technol.* **2017**, *22*, 163.
[16] A. A. Popova, S. Dietrich, W. Huber, M. Reischl, R. Peravali, P. A. Levkin, *SLAS Technol.* **2021**, *26*, 274.
[17] M. Benz, A. Asperger, M. Hamester, A. Welle, S. Heissler, P. A. Levkin, *Nat. Commun.* **2020**, *11*, 5391.
[18] N. Nagy, *Langmuir* **2019**, *35*, 5202.
[19] O. Millet, G. Gagneux, *Comptes Rendus. Mécanique* **2023**, *351*, 125.
[20] Y. Wang, S. Michielsen, H. J. Lee, *Langmuir* **2013**, *29*, 11028.
[21] N. K. Mandsberg, J. A. Serna, P. A. Levkin, *Adv. Funct. Mater.* **2024**, *34*, 2406635.
[22] N. A. Bezdenejnykh, J. Meseguer, J. M. Perales, *Phys. Fluids* **1992**, *4*, 677.
[23] A. A. Popova, K. Demir, T. G. Hartanto, E. Schmitt, P. A. Levkin, *RSC Adv.* **2016**, *6*, 38263.
[24] O. Frey, P. M. Misun, D. A. Fluri, J. G. Hengstler, A. Hierlemann, *Nat. Commun.* **2014**, *5*, 4250.
[25] A. Birchler, M. Berger, V. Jäggin, T. Lopes, M. Etzrodt, P. M. Misun, M. Pena-Francesch, T. Schroeder, A. Hierlemann, O. Frey, *Anal. Chem.* **2016**, *88*, 1222.
[26] M. Cortesi, E. Giordano, *Peer J.* **2022**, *10*, 13338.
[27] P. Kumar, A. Nagarajan, P. D. Uchil, *Cold Spring Harb. Protoc.* **2018**. http://doi.org/10.1101/pdb.prot09549710.1101/pdb.prot095497
[28] A. Montecucco, F. Zanetta, G. Biamonti, *EXCLI J.* **2015**, *14*, 95.
[29] M. C. Cox, R. Mendes, F. Silva, T. F. Mendes, A. Zelaya-Lazo, K. Halwachs, J. J. Purkal, I. A. Isidro, A. Félix, E. R. Boghaert, C. Brito, *Sci. Rep.* **2021**, *11*, 18571.
[30] B. Ayan, N. Celik, Z. Zhang, K. Zhou, M. H. Kim, D. Banerjee, Y. Wu, F. Costanzo, I. T. Ozbolat, *Commun. Phys.* **2020**, *3*, 183.
[31] A. C. Daly, M. D. Davidson, J. A. Burdick, *Nat. Commun.* **2021**, *12*, 753.
[32] I. Grexa, A. Diosdi, M. Harmati, A. Kriston, N. Moshkov, K. Buzas, V. Pietiäinen, K. Koos, P. Horvath, *Sci. Rep.* **2021**, *11*, 14813.
[33] J. Jafari, X.-L. Han, J. Palmer, P. A. Tran, A. J. O'Connor, *ACS Biomater. Sci. Eng.* **2019**, *5*, 2532.
[34] H. Byun, S. Lee, G. Nam Jang, H. Lee, S. Park, H. Shin, *Biofabrication* **2022**, *14*, 015007.
[35] M. Ingram, G. B. Techy, R. Saroufeem, O. Yazan, K. S. Narayan, T. J. Goodwin, G. F. Spaulding, *In Vitro Cell. Dev. Biol.-Animal* **1997**, *33*, 459.
[36] A. S. Chin, K. E. Worley, P. Ray, G. Kaur, J. Fan, L. Q. Wan, *Proc. Natl. Acad. Sci. USA* **2018**, *115*, 12188.

[37] C.-T. Kuo, J.-Y. Wang, Y.-F. Lin, A. M. Wo, B. P. C. Chen, H. Lee, *Sci. Rep.* **2017**, *7*, 4363.
[38] S. P. Cavnar, E. Salomonsson, K. E. Luker, G. D. Luker, S. Takayama, *J. Lab. Autom.* **2014**, *19*, 208.
[39] E. S. Place, N. D. Evans, M. M. Stevens, *Nat. Mater.* **2009**, *8*, 457.
[40] V. M. Gaspar, P. Lavrador, J. Borges, M. B. Oliveira, J. F. Mano, *Adv. Mater.* **2020**, *32*, 1903975.
[41] Y. Haraguchi, T. Shimizu, T. Sasagawa, H. Sekine, K. Sakaguchi, T. Kikuchi, W. Sekine, S. Sekiya, M. Yamato, M. Umezu, T. Okano, *Nat. Protoc.* **2012**, *7*, 850.
[42] J. A. Brassard, M. P. Lutolf, *Cell Stem Cell* **2019**, *24*, 860.
[43] M. W. Laschke, M. D. Menger, *Trends Biotechnol.* **2017**, *35*, 133.
[44] F. Birey, J. Andersen, C. D. Makinson, S. Islam, W. Wei, N. Huber, H. C. Fan, K. R. C. Metzler, G. Panagiotakos, N. Thom, N. A. O'Rourke, L. M. Steinmetz, J. A. Bernstein, J. Hallmayer, J. R. Huguenard, S. P. Pasca, *Nature* **2017**, *545*, 54.
[45] J. Luo, J. Meng, Z. Gu, L. Wang, F. Zhang, S. Wang, *Small* **2019**, *15*, 1900030.
[46] U. Mirsaidov, J. Scrimgeour, W. Timp, K. Beck, M. Mir, P. Matsudaira, G. Timp, *Lab Chip* **2008**, *8*, 2174.
[47] L. Zwi-Dantsis, B. Wang, C. Marijon, S. Zonetti, A. Ferrini, L. Massi, D. J. Stuckey, C. M. Terracciano, M. M. Stevens, *Adv. Mater.* **2020**, *32*, 1904598.
[48] J. W. Nichol, A. Khademhosseini, *Soft Matter* **2009**, *5*, 1312.
[49] R. D. Pedde, B. Mirani, A. Navaei, T. Styan, S. Wong, M. Mehrali, A. Thakur, N. K. Mohtaram, A. Bayati, A. Dolatshahi-Pirouz, M. Nikkhah, S. M. Willerth, M. Akbari, *Adv. Mater.* **2017**, *29*, 1606061.
[50] M. P. Schilling, S. Schmelzer, J. E. U. Gomez, A. A. Popova, P. A. Levkin, M. Reischl, *IEEE Access* **2021**, *9*, 166027.
[51] Y. Wu, J. E. Urrutia Gomez, H. Zhang, F. Wang, P. A. Levkin, A. A. Popova, B. Nestler, *Droplet* **2024**, *3*, 94.